Chapter 5

External kink instabilities in presence of resistive wall

5.1 Introduction

The first research on plasma stability under the existence of surrounding resistive wall was back in the paper by Kruskal *et al.* [94]. They pointed out that, in stellarators which were designed for aiming at stationary operation, the external kink mode will be destabilized due to the penetration of magnetic field in long time discharges, while it would be stabilized in a shorter time scale due to the stabilizing effect of the wall. Later, Pfirsch and Tasso [109] showed that the ideal wall has actually the stabilizing effect on external kink mode of the static plasma due to non-penetration of the magnetic field. In reality, since the surrounding wall has always small but finite resistivity, there appear slow instabilities which grow in a time scale proportional to the resistivity of the wall. The conclusion then is that, the conducting wall should not be considered as a perfect stabilizing tool for the external kink mode of static plasmas.

Goedbloed *et al.* [71] calculated the spectrum of the external kink mode for a z-pinch plasma surrounded with a resistive wall. Here a constant density and magnetic field with surface plasma current are assumed and carries surface current in equilibrium. They investigated the dependence of growth rate of kink mode on the resistivity of the wall. Since the magnetic field has no shear in this system, the Alfvén continuum is shrinked to give two point spectra propagating in the opposite direction in ideal wall case, which turns into the ideal kink mode in case of no wall. With finite resistivity of the wall, there appears a new eigenvalue on the imaginary axis of the complex ω-plane, which is now called a resistive wall mode (RWM). This mode, appearing from the origin, does not exist in the ideal wall case, and quite

resembles the behavior of the tearing mode destabilized by the resistivity of plasma itself. Other two Alfvén eigenmodes show slight damping due to the resistivity of the wall, approach to the imaginary axis, and meet each other on negative side of the imaginary axis when the resistivity is increased. If the resistivity is increased further, one of the eigenvalue on negative side of the imaginary axis moves toward negative infinity on imaginary axis, and the other constructs a pair with the one on positive side of imaginary axis, which behaves as a pair to generate the ideal kink modes.

Haney and Freidberg [80] discussed the stability of three dimensional perturbations of toroidal plasma with arbitrary cross section and current profile by using a variational principle. By introducing the effect of the resistive wall, they have extended the variational principle which is a well defined useful method for the linear stability analysis of static plasmas. It is concluded that the RWM is a purely growing mode with zero frequency, and its critical stability condition is exactly equivalent to the case with the ideal wall at infinity.

In experiments, RWMs were observed in reversed field pinch devices such as OHTE or HBTX which required the conducting wall very close to the plasma for keeping the stability [128, 34]. Since the characteristic time for the magnetic field penetration becomes long for the thick conducting wall, RWM is relatively easily suppressed. However, it becomes shorter than the discharge period when the conducting wall is thin. Thus, some discharges are terminated by the growth of this mode. These results are considered to coincide with theoretical predictions of RWMs for static equilibria.

Recently, the stabilization of RWM was experimentally discovered at DIII-D tokamak in early 90's [135, 121, 122]. According to the experimental results, this mode did not appear for longer discharge period than the time scale of the resistive wall even for the higher β value than the threshold of external kink modes. In DIII-D, plasmas are rotating in the toroidal direction due to the tangential neutral beam injection. Therefore, this plasma rotation was considered as the stabilizing effect on the RWM.

Numerical calculation by Bondeson and Ward was the first theoretical investigation for this topic [44, 147]. With an eigenvalue code including both the resistive wall and the toroidal rigid rotation, they showed that the kink mode belonging to the shear Alfvén branch is stabilized by the sound wave resonance generated by the plasma rotation in the toroidal plasma. Betti and Freidberg has shown the existence of the coupling even in cylindrical geometry, and also concluded that the RWM can be stabilized by the sound wave resonance [41]. Moreover, several other stabilizing mechanisms such as resonance due to Alfvén continuous spectra [153], resonance

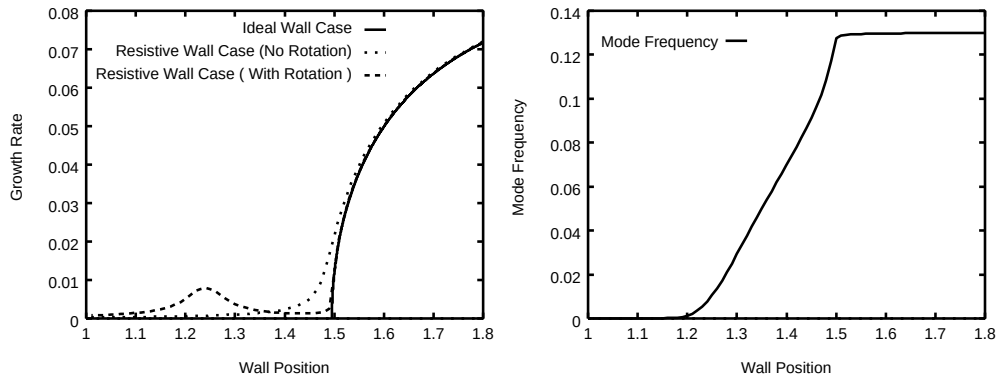

Figure 5.1: Dependence of growth rate or real frequency of the RWM in a cylindrical plasma with rigidly axial flow on the position of resistive wall. Growth rate and frequency are normalized by the poloidal Alfvén time, and the wall position is normalized by plasma radius.

due to cusp continuous spectra [42], resistivity [62] , or viscosity [64], were studied; however, there is no clear correlation to the experimental results. In addition, from the theoretical point of view, mathematical theory is not completed for the effect of continuous spectra or non-Hermiticity of the operator on the stability problem. Instead of solving this difficult problem, many theoretical studies are related to the feedback control of dangerous mode or mode locking phenomena [70, 89, 63, 154].

In this chapter, we will focus on the appearance of non-Hermiticity for the linear instability of the external kink mode under the existence of surrounding resistive walls and rigid plasma flows. As a reference, typical growth rate dependence on the position of the resistive wall relative to the plasma radius is shown in Fig. 5.1 [153]. This figure the obtained for a cylindrical plasma with a rigid axial flow. With the ideal wall placed closer to the plasma column, the ideal external kink mode is stabilized (solid line); however, for the resistive wall, the instability still remains in a time scale of the resistive diffusion of magnetic field in the wall, which is called the resistive wall mode or RWM. The growth rate of the RWM is monotonically increasing and becomes almost equal to that of the ideal external kink mode when the wall position is far from the plasma column if the plasma has no axial flow (dotted line). However, if we introduce the rigid flow (dashed line), the growth rate becomes large once at $c/a \sim 1.2$, where c (a) denote the radius of the resistive wall (plasma column). This small hump is observed in almost all calculations of growth rate of RWM, e.g. Bondeson and Ward [44, 147], Betti and Freidberg [41], Finn [62], and Fitzpatrick and Aydemir [64], and it seems that the wall position corresponding to this small hump determines the closest threshold of the wall position for stabilizing RWM. Nevertheless, no physical or mathematical discussion for the appearance of

the small hump in Fig. 5.1 is found in literatures. From the plot of real frequency for the case of rigidly flowing plasma (right side figure of Fig. 5.1), RWM is locked to the wall in the region $c/a \lesssim 1.2$. It begins to slip with respect to the wall at $c/a \simeq 1.2$, and has the finite frequency for $c/a \gtrsim 1.2$. Therefore, it is conjectured that the non-Hermiticity plays an important role in the behavior of RWM. Also our interest is in the mechanism for the appearance of the hump in the growth rate shown in the left side figure of Fig. 5.1.

We will first show that the Kelvin-Helmholtz instability, which is well known in fluid dynamics as an instability driven by a shear flow, could be described as an interaction of two out-of-phase surface waves in Sec. 5.2. The rest of this chapter is devoted for the detailed study the RWM. We will give the governing equations, then discuss the difficulty in constructing exact mathematical theory in Sec. 5.3. Instead of constructing the complete solutions of the system, we focus on the similarity to the Kelvin-Helmholtz instability, we will introduce a surface current model in Sec. 5.4. With the aid of this simplification, we have given a model with focusing on the non-Hermiticity of RWM. The detailed analysis will be given in Sec. 5.5. We will summarize the obtained results in Sec. 5.6.

5.2 Non-Hermiticity of Kelvin-Helmholtz instability

In this section, we will show that Kelvin-Helmholtz instability, which is one of the most well-known instabilities in fluid dynamics arising from non-Hermiticity of the generator, can be represented in a closed form describing an interaction of two surface waves. We will revise here the piecewise linear shear flow model used in Refs. [134, 73, 7].

For the y directed ambient flow which is sheared in the x direction, the perturbed vorticity of two dimensional incompressible Euler fluid is written in the form of Rayleigh equation:

$$\mathrm{i}\partial_t \Psi = [k v_0(x) + k v_0''(x)\, \mathcal{K}]\, \Psi, \tag{5.1}$$

where the perturbed vorticity $\Psi(x,t)$ and the integral operator $\mathcal{K}$ are expressed as

$$\Psi(x,t) = -\Delta\phi(x,t), \tag{5.2}$$

$$\mathcal{K}\Psi \equiv -\Delta^{-1}\Psi = \frac{1}{2k}\int e^{-k|x-\xi|}\, \Psi(\xi,t)\, \mathrm{d}\xi, \tag{5.3}$$

and ϕ and k denote a stream function and a wave number in the y direction, respectively. Here, $\Delta = \partial_x^2 + \partial_y^2$ denotes the two dimensional Laplacian operator.

Hereafter, we will investigate properties of the operator

$$\mathcal{A} = kv_0(x) + kv_0''(x)\mathcal{K} \tag{5.4}$$

in the infinite domain. It is noted that the non-Hermiticity of this operator is originated from the non-commutativity of two Hermitian operators, the multiplication $v_0''(x)$ and the inverse Laplacian $\mathcal{K}$. Actually, if $v_0''(x)$ does not change its sign over the domain, we can define a norm by introducing a weight function $1/|v_0''(x)|$ and construct a Hermitian operator in such normed domain [38]; however, the Kelvin-Helmholtz unstable system should have an inflection point of $v_0(x)$ [111], and thus, this instability should be considered to be cause by the non-Hermiticity of the operator $kv_0''(x)\mathcal{K}$.

Let us first consider the linear ambient velocity profile

$$v_0(x) = \frac{U}{a}x, \quad (-\infty < x < \infty). \tag{5.5}$$

Since the operator $\mathcal{A}$ is Hermitian due to $v_0''(x) = 0$, it has the continuous spectrum λ ($\in \mathbb{R}$) and the corresponding singular eigenfunction is

$$\varphi = \delta(x - \mu), \tag{5.6}$$

where $\mu = a\lambda/kU$. Here we will pick up the following two eigenfunctions from the continuous spectrum

$$\varphi_1 = \delta(x - a), \quad \varphi_2 = \delta(x + a), \tag{5.7}$$

for later discussions. Taking these eigenfunctions as basis vectors for the linear subspace, the operator will be expressed in terms of these vectors as

$$\mathcal{A} = \begin{pmatrix} kU & 0 \\ 0 & -kU \end{pmatrix}, \tag{5.8}$$

which is a diagonal matrix.

Next, let us consider the equilibrium shear flow in which the velocity profile is assumed to be constant in $x \leq -a$ and $x \geq a$ as illustrated in Fig. 5.2;

$$v_0(x) = \begin{cases} -U & (x \leq -a) \\ Ux/a & (-a < x < a) \\ U & (a \leq x) \end{cases}. \tag{5.9}$$

In this case, $v_0''(x)$ is expressed by the two delta function placed at $x = \pm a$, and the operator is found to be non-Hermitian. Two eigenfunctions in Eq. (5.7) will be modified and yield

$$\tilde{\varphi}_1 = \delta(x - a) + A\delta(x + a), \tag{5.10}$$

$$\tilde{\varphi}_2 = A\delta(x - a) + \delta(x + a), \tag{5.11}$$

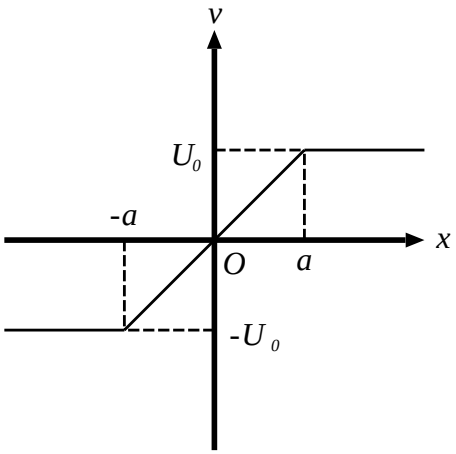

Figure 5.2: A model equilibrium velocity profile unstable against Kelvin-Helmholtz instability.

where A denotes

$$A = (2ka-1)e^{2ka} + \sqrt{(2ka-1)^2 e^{4ka} - 1}. \tag{5.12}$$

When the ambient velocity profile is snapped, two independent surface waves (φ_1 and φ_2) couple each other and they constitute new eigenstates ($\tilde{\varphi}_1$ and $\tilde{\varphi}_2$). The eigenvalues corresponding to them are

$$\tilde{\lambda}_1 = -\frac{U}{2a}\sqrt{(2ka-1)^2 - e^{-4ka}}, \tag{5.13}$$

$$\tilde{\lambda}_2 = \frac{U}{2a}\sqrt{(2ka-1)^2 - e^{-4ka}}, \tag{5.14}$$

respectively. One of them with the eigenvalue $\tilde{\lambda}_1$ corresponding to the eigenfunction $\tilde{\varphi}_1$ turns out to be unstable if the condition

$$(2ka-1)^2 < e^{-4ka} \tag{5.15}$$

is satisfied. Here we have defined $\sqrt{\alpha-\beta} = \mathrm{i}\sqrt{\beta-\alpha}$ for $\alpha < \beta$.

The singular function $\varphi_\mu = \delta(x-\mu)$ $(-a < \mu < a)$, which is the eigenfunction when the ambient velocity profile was completely linear in the whole space, will be modified here as

$$\tilde{\varphi}_\mu = B_-\delta(x-a) + \delta(x-\mu) + B_+\delta(x+a), \tag{5.16}$$

although the eigenvalue does not change, where

$$B_\pm = \frac{[2k(a\pm\mu)-1]e^{-k(a\mp\mu)} + e^{-k(a\pm\mu)}\,e^{-2ka}}{[2k(a-\mu)-1][2k(a+\mu)-1] - e^{-4ka}}. \tag{5.17}$$

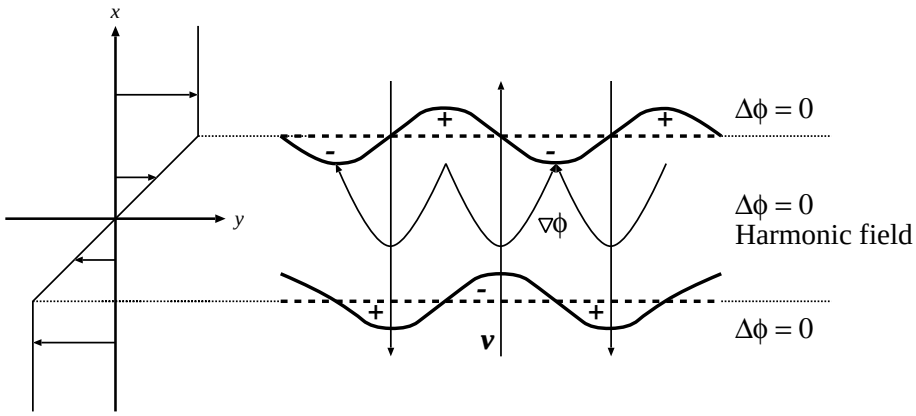

Figure 5.3: Schematic pictures of Kelvin-Helmholtz instability. The piecewise linear line in the left figure denotes the ambient velocity profile. It has the snapping point at $x = \pm a$ and the perturbed vorticity will be excited there which is denoted in the right figure by the wavy line.

If μ satisfies

$$\mu = \pm\sqrt{(2ka-1)^2 - e^{-4ka}}, \tag{5.18}$$

then $\tilde{\varphi}_\mu$ will not be defined by the above expression and the system has a possibility of resonance. However, if we consider the Kelvin-Helmholtz unstable system, the right hand side of Eq. (5.18) becomes purely imaginary from the condition (5.15), and we do not need to care about the resonance. This problem will be discussed more carefully in Chap. 7.

Thus, by taking the eigenfunctions $\tilde{\varphi}_1$, $\tilde{\varphi}_\mu$, and $\tilde{\varphi}_2$ as basis vectors for the linear subspace, the operator will be expressed in terms of these vectors as

$$\mathcal{A} = \frac{U}{2a}\begin{pmatrix} 2ka-1 & -e^{-k(a-\mu)} & -e^{-2ka} \\ 0 & 2k\mu & 0 \\ e^{-2ka} & e^{-k(a+\mu)} & -(2ka-1) \end{pmatrix}, \tag{5.19}$$

under the condition (5.15). Although this matrix may look to have a form of Jordan type with the coincidence of its diagonal elements, when $\pm(2ka-1) = 2k\mu$ is satisfied, it is semi-simple type and can be diagonalized. The important point here is that, the singular eigenfunction does not affect the coupled surface waves, and the instability is independent of the continuous spectrum.

Schematic pictures of the mechanism of Kelvin-Helmholtz instability are illustrated in Fig. 5.3. Physically, two surface waves, which are excited at the place where the ambient velocity profile is snapped, are coupled each other to construct the eigenstate. When the system is Kelvin-Helmholtz unstable, it is noted that the relative amplitude A becomes complex and $|A| = 1$ from Eq. (5.12). Namely they

have the same amplitude with out of phase and are connected by the harmonic field

$$\Delta\phi = 0, \tag{5.20}$$

in the region between two snapped points of $v_0(x)$ $[v_0''(x) = 0]$. Therefore, the gradient field of the stream function points from positive vorticity position to the negative one in the same way as that (electric field) of the electrostatic potential produced by the electric charge. Since the perturbed velocity is orthogonal to the gradient field of the stream function,

$$\boldsymbol{v} = \nabla\phi \times \boldsymbol{e}_z, \tag{5.21}$$

it affects on the other surface to amplify the original disturbance, and vice versa.

Therefore, the mechanism of Kelvin-Helmholtz instability could be understood as a positive feedback between two coupled surface waves, and it could be represented in a closed form of the interaction of such surface waves. Kelvin-Helmholtz instability is shown to be caused by the interaction of two out-of-phase surface waves with the same amplitude which are placed at $x = \pm a$ $[v_0''(x) \neq 0]$.

5.3 Model equations for resistive wall mode

Here we will regard the RWM as a current driven, ideal external kink mode in a low β plasma for simplicity. By neglecting the plasma resistivity, the linearized reduced MHD equations for a static incompressible low β plasma are shown as (see Chap. 2)

$$\partial_t \Delta\phi = \frac{1}{\mu_0\rho_0}\left(\boldsymbol{B}_0 \cdot \nabla\Delta\psi + \boldsymbol{B}_1 \cdot \nabla\Delta\psi_0\right), \tag{5.22}$$

$$\partial_t \psi = \boldsymbol{B}_0 \cdot \nabla\phi. \tag{5.23}$$

Combining them yields

$$\partial_t^2 \psi = \frac{1}{\mu_0\rho_0}(\boldsymbol{B}_0 \cdot \nabla\Delta^{-1}\boldsymbol{B}_0 \cdot \nabla\Delta\psi + \boldsymbol{B}_0 \cdot \nabla\Delta^{-1}\boldsymbol{B}_1 \cdot \nabla\Delta\psi_0), \tag{5.24}$$

where ϕ and ψ denote the stream function and the poloidal flux function, respectively.

On the other hand, by writing the wall permeability and resistivity as μ_w and η_w, the simple diffusion equation,

$$\partial_t \psi = \frac{\eta_\mathrm{w}}{\mu_\mathrm{w}}\Delta\psi, \tag{5.25}$$

holds in the resistive wall. Since the order of time derivative differs between the evolution equation of the plasma and that of the resistive wall, we formally adjust

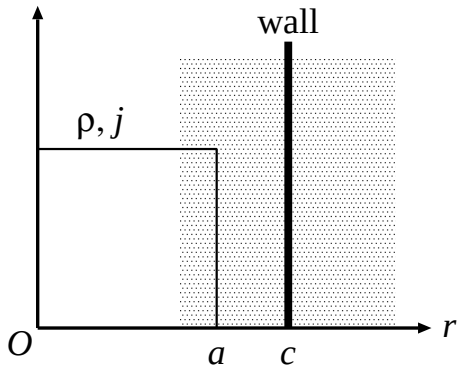

Figure 5.4: The profile of density and current of the cylindrical plasma.

the order of them by taking the time derivative on both side of Eq. (5.25) and combine these equations as

$$\partial_t^2 \psi = \frac{\chi}{\mu_0 \rho_0} \left[\boldsymbol{B}_0 \cdot \nabla \Delta^{-1} \boldsymbol{B}_0 \cdot \nabla \Delta \psi - \mathcal{L}_{\mathrm{K}} \psi \right] + \chi^* (\varepsilon \partial_t \Delta \psi - \partial_t \boldsymbol{v}_0 \cdot \nabla \psi), \qquad (5.26)$$

where we have introduced the driving operator of the kink instability $\mathcal{L}_{\mathrm{K}}\psi = \boldsymbol{B}_0 \cdot \nabla \Delta^{-1} \boldsymbol{B}_1 \cdot \nabla \Delta \psi_0$, χ is the function which has the value 1 in the plasma and 0 in the resistive wall, respectively, and vice versa for χ^*. We have assumed that the plasma is rigidly moving in the axial direction with velocity $\boldsymbol{v}_0$ with respect to the wall, and Eq. (5.26) is written in the rest frame of the plasma. In Eq. (5.26), $\varepsilon = \eta_{\mathrm{w}}/\mu_{\mathrm{w}}$.

In this formal evolution equation, the time derivative is included in the right hand side. It is because the resistive wall has its own time scale which is different from that of the plasma, and it reacts differently depending on the frequency of fluctuations. That is, the magnetic fluctuation cannot deeply penetrate into the wall if the frequency of the fluctuation is high, and the wall behaves as the conductor with less penetrativity, while it behaves as vacuum-like with allowing the magnetic field penetration more easily if the frequency is very low. Therefore, with the above formal evolution equation, it is very difficult to evaluate the mirror current directly by keeping the time derivative. We will study behavior of eigenmodes by assuming the exponential dependence $\psi \propto e^{\gamma t}$ for fluctuations.

5.4 Surface current model

Consider a one dimensional straight cylindrical plasma with radius a surrounded by a concentric conducting wall whose radius and thickness are c ($> a$) and δ ($\ll a$), respectively. Profiles of density and current of the plasma are assumed to be constant as in Fig. 5.4. In this case, wave numbers m and k_z in azimuthal (θ)

and axial (z) directions become good quantum numbers, which reduces Eq. (5.24) and yield

$$\left(1+\frac{\mu_0\rho_0\gamma^2}{F^2}\right)\Delta\psi=\frac{m\mu_0 j_0'(r)}{rF(r)}\psi, \tag{5.27}$$

where $F=mB_{0\theta}/r+k_zB_{0z}$ with the subscript 0 denoting the equilibrium quantity. Prime denotes the derivative with respect to radial coordinate r, and γ denotes the aforementioned time constant (growth rate). Hereafter, we will omit the subscript 1 denoting perturbations for simplicity. Since the safety factor is assumed constant in the whole plasma, the Alfvén velocity does not vary in space. Therefore, Alfvén continuum is shrinked to give point spectra in this system.

Under these assumptions, the system gives just Laplace equation

$$\Delta\psi=0, \tag{5.28}$$

both in plasma ($r<a$) and in vacuum ($r>a$) [62]. A dispersion relation is given by the connection conditions at the plasma edge and the resistive wall which lead to

$$\psi'(a+)-\left(1+\frac{\mu_0\rho_0\gamma^2}{F^2}\right)\psi'(a-)=-\frac{m\mu_0 j_0}{aF}\psi(a), \tag{5.29}$$

$$\left.\frac{\mathrm{d}\psi}{\mathrm{d}r}\right|_{c+}-\left.\frac{\mathrm{d}\psi}{\mathrm{d}r}\right|_{c-}=\frac{\bar{\gamma}\tau_{\mathrm{w}}}{c}\psi(c), \tag{5.30}$$

where $\tau_{\mathrm{w}}=c\delta\mu_{\mathrm{w}}/\eta_{\mathrm{w}}$ and δ denotes the thickness of the wall. Here we have used the solutions of vacuum region ($a<r<c$) and inside the wall region ($c<r<c+\delta$), which are expressed with $r^{\pm m}$ and the Bessel functions, respectively. For the thickness of the wall, $\delta\ll c$ is assumed. It is noted that, since the equations are written in the rest frame of the plasma, the connection condition (5.30) contains the Doppler shifted mode growth rate $\bar{\gamma}\equiv\gamma+\mathrm{i}\Omega$, where $\Omega=\boldsymbol{k}\cdot\boldsymbol{v}_0$ denotes the axial flow velocity of the plasma column normalized by the wave number. The eigenfunction describing the surface current at the plasma edge and at the wall has a physical meaning that the plasma surface current tends to be kink unstable, while the wall surface current tends to suppress it.

Since the inner region (resistive wall) equation is described by the field diffusion equation, the formulation is rather simple here comparing with the resistive instabilities which contains the resistivity of the plasma itself [68, 4, 5, 24]. The time scale of RWM is proportional to the resistive skin time of the wall, while resistive instabilities are described by some fractions of the combination of resistivity and Alfvén time due to the coupling of the plasma motion and resistivity even inside the inner region.

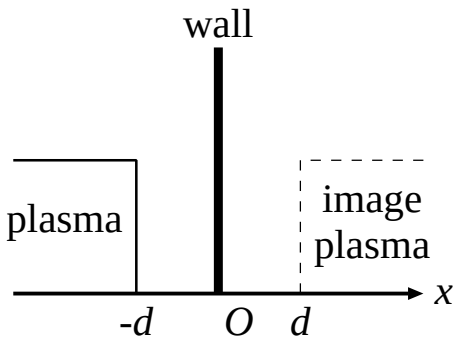

Figure 5.5: A slab model for the calculation of mirror image current.

5.5 Non-Hermiticity of resistive wall mode

In this section, we will discuss the non-Hermiticity on the linear stability problem of RWMs. We have shown in Sec. 5.2 that, as an example for the treatment of non-Hermitian operator, the Kelvin-Helmholtz instability could be described by an interaction of two out-of-phase surface waves with the same amplitude. We will show here that the RWM could also be described as an interaction of two out-of-phase surface waves with the same amplitude in a certain situation.

5.5.1 Calculation of image current in slab geometry

In order to make a comparison between image current and plasma surface current, we will stretch and approximate the shaded region in Fig. 5.4 by a slab geometry as shown in Fig. 5.5. If the radial characteristic length, $1/k_r$, of the unstable mode is much smaller than the radius of the plasma column ($k_r a \gg 1$), we can approximate even the plasma region by a slab geometry with keeping the kink driving term. We will take the origin $x = 0$ at a position of the wall, and assume the plasma to be confined at $x \leq -d$. The connection conditions (5.29) and (5.30) are then written as

$$\psi'(-d+) - \left(1 + \frac{\mu_0 \rho_0 \gamma^2}{F^2}\right) \psi'(-d-) = -\frac{k\mu_0 j_0}{F} \psi(-d), \tag{5.31}$$

$$\left.\frac{\mathrm{d}\psi}{\mathrm{d}x}\right|_{0+} - \left.\frac{\mathrm{d}\psi}{\mathrm{d}x}\right|_{0-} = \frac{\bar{\gamma}\tau_{\mathrm{w}}}{d} \psi(0), \tag{5.32}$$

where $\tau_{\mathrm{w}} = d\delta\mu_{\mathrm{w}}/\eta_{\mathrm{w}}$.

No wall case If the system does not have any conducting wall, the eigenstate is expressed by the surface current flowing on plasma edge;

$$j = \delta(x + d), \tag{5.33}$$

where the corresponding eigenvalue is evaluated as

$$\gamma^2 = \frac{F}{\mu_0 \rho_0}(\mu_0 j_0 - 2F). \tag{5.34}$$

The first term in the expression of the growth rate denotes the destabilizing effect due to the plasma current, and the second one denotes the stabilizing effect due to the Alfvén wave, respectively. Hereafter, we assume for the normalization that the coefficient of the surface current perturbation given by the δ function at the plasma edge to be unity as in Eq. (5.33).

Ideal wall case By assuming the ideal conducting wall at $x = 0$, the boundary condition becomes

$$\tilde{\psi}|_{x=0} = 0, \tag{5.35}$$

which can be represented by assuming the wall current

$$j_{\mathrm{w}} = -e^{-kd}\delta(x). \tag{5.36}$$

The wall current at $x = 0$ can be moved to $x = d$ with keeping the same magnetic field in $x < 0$ as

$$j_{\mathrm{im}}^{(\mathrm{i})} = -\delta(x - d). \tag{5.37}$$

Since the ideal wall does not have its own time constant, it reacts in the same way as for any frequency of magnetic perturbation. Thus, the mirror image current flows in the opposite direction with the same amplitude as the surface current of plasma which is independent of the frequency. Then, corresponding eigenvalues are given by

$$\gamma^2 = \frac{F}{\mu_0 \rho_0}\Big(\mu_0 j_0 - \frac{2F}{1 - e^{-2kd}}\Big). \tag{5.38}$$

Comparing with Eq. (5.34), the effect of conducting wall appears in the second stabilizing term here, which becomes larger than the previous no wall case. Hereafter, we will mainly consider the following parameter regime

$$\frac{2F}{\mu_0} < j_0 < \frac{2F}{\mu_0(1 - e^{-2kd})}, \tag{5.39}$$

where the external kink mode is unstable without the wall [Eq. (5.34)], while for the case with the ideal wall [Eq. (5.38)], it is stable.

Resistive wall case If we put the resistive wall at $x = 0$, the connection condition

$$\left.\frac{\mathrm{d}\tilde{\psi}}{\mathrm{d}x}\right|_{0+} - \left.\frac{\mathrm{d}\tilde{\psi}}{\mathrm{d}x}\right|_{0-} = \frac{\bar{\gamma}\tau_{\mathrm{w}}}{d}\tilde{\psi}(0), \tag{5.40}$$

will be replaced by the following mirror image current;

$$j_{\mathrm{im}}^{(\mathrm{r})} = -\left(1 + \frac{2kd}{\bar{\gamma}\tau_{\mathrm{w}}}\right)^{-1}\delta(x-d), \tag{5.41}$$

instead of Eq. (5.37). Note that the amplitude and phase of the image current now depends on the time constant of the unstable mode.

With the Alfvén time $\tau_{\mathrm{A}}^2 = \mu_0\rho_0/F^2$, the growth rate γ and axial flow frequency Ω are normalized as

$$\hat{\gamma} = \gamma\tau_{\mathrm{A}}, \quad \hat{\Omega} = \Omega\tau_{\mathrm{A}}. \tag{5.42}$$

By further introducing $\epsilon = \tau_{\mathrm{A}}/\tau_{\mathrm{w}}$ as an expanding parameter, the dispersion relation leads to the third order algebraic equation in the form of

$$A\hat{\gamma}^2(\hat{\gamma} + \mathrm{i}\hat{\Omega}) + \epsilon B\hat{\gamma}^2 + C(\hat{\gamma} + \mathrm{i}\hat{\Omega}) + \epsilon D = 0, \tag{5.43}$$

where

$$\begin{aligned} A &= 1 - e^{-2kd}, \\ B &= 2kd, \\ C &= \left[2 - \frac{\mu_0 j_0}{F}(1 - e^{-2kd})\right], \\ D &= 2kd\left(2 - \frac{\mu_0 j_0}{F}\right). \end{aligned}$$

Let us check the sign of them for the following analysis; $A > 0$ and $B > 0$ are always valid. From the condition (5.39), it can be concluded that $D < 0$ holds since the external kink mode is unstable without the wall, and that $C > 0$ holds since it is stabilized by introducing the ideal wall. In summary, the signs of the coefficients in the dispersion relation (5.43) satisfy

$$A > 0, \quad B > 0, \quad C > 0, \quad D < 0, \tag{5.44}$$

in our parameter regime.

5.5.2 Behavior of eigenvalue and eigenvector of resistive wall mode

Let us solve analytically the dispersion relation (5.43) by means of perturbation method under $\epsilon \ll 1$. In the following, we will omit the hat on the eigenvalues for

simplicity. By expanding the eigenvalue as

$$\gamma = \gamma_0 + \epsilon\gamma_1 + \cdots, \tag{5.45}$$

we have three solutions in $O(1)$ as

$$\gamma_0 = \pm \mathrm{i}\sqrt{\frac{C}{A}}, -\mathrm{i}\Omega. \tag{5.46}$$

Taking the next order in $O(\epsilon)$, they are written as

$$\gamma^{(0)} = -\mathrm{i}\Omega - \epsilon\frac{B\Omega^2 - D}{A\Omega^2 - C}, \tag{5.47}$$

$$\gamma^{(\pm)} = \pm\mathrm{i}\sqrt{\frac{C}{A}} \mp \epsilon\frac{BC - AD}{2A\sqrt{C}(\pm\sqrt{C} + \sqrt{A}\Omega)}. \tag{5.48}$$

Due to the signs of the coefficients shown in Eq. (5.44), we see that $B\Omega^2 - D > 0$ and $BC - AD > 0$ hold. Moreover, since $A\Omega^2 - C$ gives

$$\lim_{kd\to 0}(A\Omega^2 - C) = -2, \tag{5.49}$$

$\gamma^{(0)}$ gives the unstable solution for small kd, while other two roots $\gamma^{(\pm)}$ give the damped oscillations. However, it can be seen from Eqs. (5.47) and (5.48) that the denominator of γ_1 has zero while the numerator keeps $B\Omega^2 - D > 0$ from the conditions $B > 0$ and $D < 0$.

It means that the perturbation expansion breaks down in the regime $A\Omega^2 - C \sim O(\epsilon^{-1})$. The position of the wall which gives zero of the denominator will be evaluated by solving $A\Omega^2 - C \sim 0$ for kd as

$$kd \sim -\frac{1}{2}\log\Big[1 - 2\Big(\Omega^2 + \frac{\mu_0 j_0}{F}\Big)^{-1}\Big]. \tag{5.50}$$

After exceeding this value and $A\Omega^2 - C \sim O(1)$ holds again, then $\gamma^{(0)}$ turns out to show damping and $\gamma^{(-)}$ represents unstable RWM which relates to the ideal external kink mode. On the other hand, $\gamma^{(+)}$ shows always damping, and it does not have any break down of the perturbation method.

In order to investigate the detailed behavior of eigenmodes near the wall position expressed in Eq. (5.50), we will show the numerical results of Eq. (5.43) in Figs. 5.6 and 5.7. Analytic solutions $\gamma^{(0)}$ and $\gamma^{(-)}$ are also plotted in them. Numerical calculation is carried out for the parameter $\tau_\mathrm{w}/\tau_\mathrm{A} = 10^4$, $\mu_0 j_0/F = 2.01$, and $\Omega = 0.15$. In this case, the stabilizing parameter regime for the external kink mode with the surrounding ideal wall is evaluated from Eq. (5.39) as

$$kd \lesssim 2.65. \tag{5.51}$$

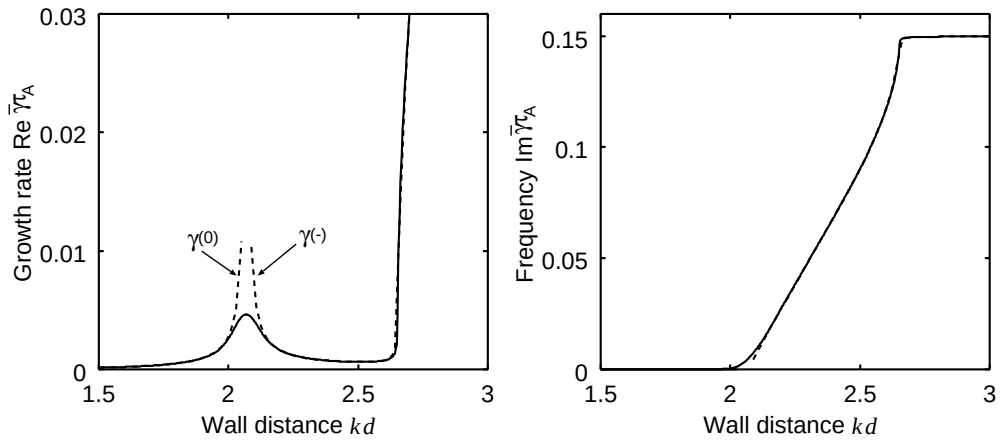

Figure 5.6: Real and imaginary part of the eigenvalue of the dispersion relation (5.43), which corresponds to the unstable RWM.

The large growth rate for the wall position $kd \gtrsim 2.65$ in Fig. 5.6 corresponds to the ideal external kink mode. For the imaginary part of the eigenvalue (frequency), it is seen that the external kink mode moves together with the plasma for $kd \gtrsim 2.65$. The wall position corresponding to the break down of the perturbation expansion is evaluated from Eq. (5.50) as

$$kd \sim 2.07. \tag{5.52}$$

As described in Sec. 5.1, we see in Fig. 5.6 that a small hump of the growth rate in the kink stable region (5.51) of the wall position approximately coincides with the break down point of the perturbation expansion [Eq. (5.52)].

With the numerical solutions, we have evaluated the amplitude and phase of the mirror image current compared to the plasma surface current by using Eq. (5.41) (see Fig. 5.7). It is seen that the amplitude of the image current becomes smaller when they are closer, while the interaction of two surface waves becomes stronger then. Therefore, the RWM in the wall position closer than the value (5.52) is caused by the decrease of the image current which has the effect to stabilize the external kink mode by suppressing the perturbed plasma surface current [10]. However, it is not the case with the wall position $kd \gtrsim 2$.

It is found that the amplitude of the image current is almost unity for the wall position $kd \gtrsim 2$ in Fig. 5.7. Moreover, it is clearly seen from Fig. 5.7 that the phase shift is quite localized at the wall position where the perturbation expansion breaks down, which has not been obtained by the analytic solution $\gamma^{(0)}$. The phase shift is evaluated to be relatively small, i.e. few degrees, which comes from the smallness of the expansion parameter $\epsilon \sim 10^{-4}$. Even for the small but finite phase shift, the interaction of two surface waves in the RWM contains a similar effect to the Kelvin-

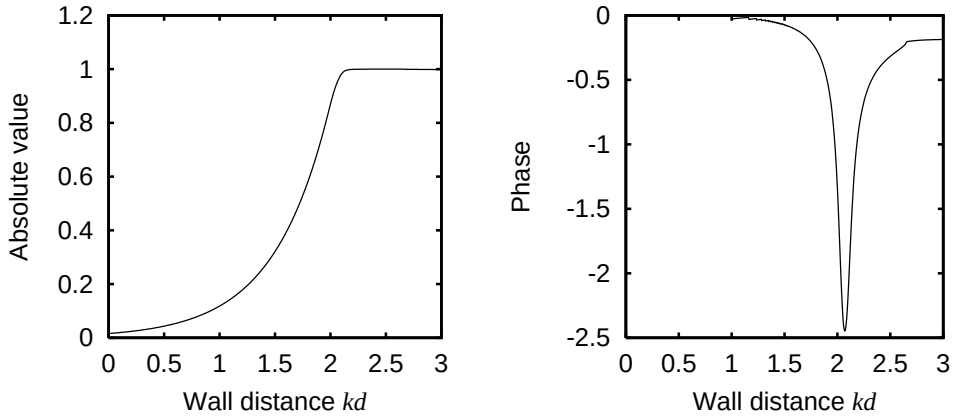

Figure 5.7: Amplitude and phase of the mirror image current relative to plasma surface current obtained with Eq. (5.41). The phase is described in the unit of degree.

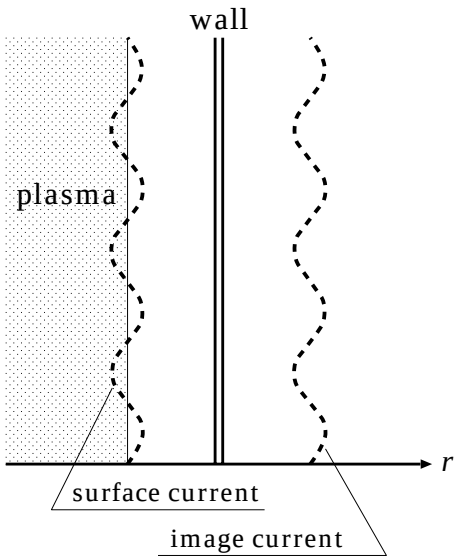

Figure 5.8: Schematic view of the destabilizing mechanism of RWM.

Helmholtz instability, which is another destabilizing mechanism for the RWM as shown in Fig. 5.8.

5.6 Summary

In this chapter, we have analyzed the resistive wall mode (RWM) in the rigidly flowing plasma surrounded by the conducting wall and investigated the situation where non-Hermiticity plays an important role for the destabilization mechanism.

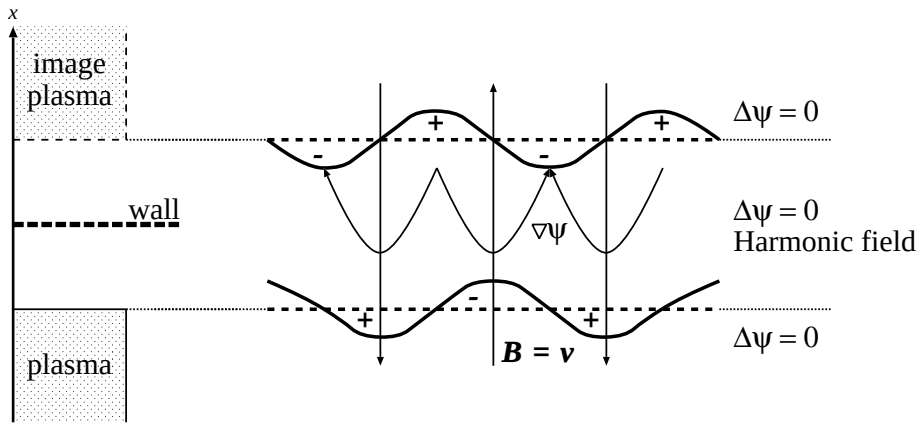

Figure 5.9: Physical mechanism of the destabilizing effect of the RWM. Two surface waves are connected by the harmonic field, which is the same as the Kelvin-Helmholtz instability in neutral fluids.

When the plasma is static with respect to the resistive wall, the amplitude of mirror image current is small due to resistivity, and has the same phase as that of the plasma surface current. When the plasma is rigidly flowing with respect to the resistive wall, the phase shift arises between the plasma surface current and the mirror image current, which brings about the destabilization with a positive feedback mechanism in the same way as Kelvin-Helmholtz instability in neutral fluids. This destabilizing effect creates the small hump of the growth rate depending on the wall position (see Figs. 5.1 and 5.6).

We have derived a third order algebraic dispersion relation of RWM for a simplified slab model, and solved it analytically by means of perturbation expansion as Eqs. (5.47) and (5.48). Analytic solution $\gamma^{(0)}$ does not contain any phase shift, however, we found that the perturbation expansion breaks down due to zero of the denominator at a certain wall position [Eq. (5.50)]. By numerically solving the dispersion relation, the eigenvalue $\bar{\gamma}$ becomes a complex number for the break down condition, which actually gives a substantial phase shift between plasma surface current and mirror image current.

The destabilizing mechanism of RWM can be qualitatively explained as follows. In the situation illustrated in Fig. 5.5, the system has a homogeneous current density j_{0z} in the region $x < -d$ and $d < x$. When we distort the surfaces at $x = \pm d$ as illustrated in Fig. 5.9, positive and negative localized surface current streets are alternatively produced with the wave form. Let us consider the effect of upper surface current on the lower one in the situation shown in Fig. 5.9. Since the region between the two surface current streets are vacuum, the eigenmode of the magnetic

fluctuation satisfies the Laplace equation

$$\Delta\psi = 0, \tag{5.53}$$

in this region. Therefore, harmonic field of the perturbed flux function ψ appears between the two surface current streets. The gradient field $\nabla\psi$ governs the structure of magnetic perturbation as illustrated in Fig. 5.9. Since the magnetic fluctuation is expressed by

$$\boldsymbol{B} = \nabla\psi \times \boldsymbol{e}_z, \tag{5.54}$$

where $\boldsymbol{B}$ is perpendicular to the field $\nabla\psi$ in the xy-plane. For the Alfvén wave branch, since the plasma is frozen in the magnetic field, the direction of the perturbed magnetic field is parallel to the velocity field, whose profile corresponds to the amplification of the accompanying out-of-phase surface current. The lower surface current in Fig. 5.9 will produce the velocity field which amplifies the upper one, and vice versa. Thus, these two surface waves become unstable by amplifying each other.

In previous papers, when the system contains any continuous spectra, it is expected that the RWM is stabilized due to the rigid flow for the outer wall position than that corresponding to the small hump of the growth rate. Therefore, it may be concluded that the resistive wall should be placed at somewhat outer position than that expressed by Eq. (5.50) in order to obtain the stabilizing effect. The expression (5.50) shows that, if the flow velocity is increased, kd becomes small and closer to zero. This means that the wall position which gives the extremum of the growth rate will become closer to the plasma edge; however, the dependence is weak as is expressed from the logarithmic function. Thus, the flow velocity of the plasma does not affect the result significantly.